Nb/Al-AlO_x/Nb junction properties' variations due to storage and mounting

A. Pavolotsky, D. Dochev, V. Belitsky *Senior Member, IEEE*

***Abstract*—We report studies of room temperature aging and annealing of Nb/Al-AlO_x/Nb tunnel junctions with a $2\ldots3\,\mu m^2$ size. We observed a noticeable drop of the junction normal resistance R_n unusually combined with increase of subgap resistance R_j as a result of aging. Changes of R_j occur at sufficiently shorter time scale than that of R_n. Variation of both R_n and R_j depend on the junction size. An effect of aging history on the junction degradation after consequent annealing was discovered. We suggest that the observed junction aging and annealing behavior could be explained by diffusional ordering and structural reconstruction in the tunnel AlO_x barrier. The diffusion driving such structural ordering and reconstruction of the AlO_x tunnel layer is enhanced due to the intrinsic stress relaxation (creep) processes in the underlying *Al* layer. Also, we discuss the influence of dicing the wafer into the single mixer chip on the junction aging behavior.**

***Index Terms*—Superconducting devices, superconducting tunnel junctions, superconducting device reliability, superconducting device thermal stability**

I. Introduction

FOR many applications [1], [2], long-term stability of the of *Nb-SIS* junction properties has a particular importance. During the projected service time (e.g., up to 20 years for ALMA), junctions may experience long storage periods at room conditions, multiple thermal cycling and possible re-mounting, the latter requiring exposure to moderate elevated temperatures. For years, since introduction of Nb/Al-AlO_x/Nb tunnel junctions [3], [4], variation of their properties under room temperature aging and annealing at elevated temperatures has been extensively discussed [5]–[12]. However, no consistent explanation for the observed effects has been proposed. This work presents some new experimental results along with a new interpretation of the properties and its changes for the Nb/Al-AlO_x/Nb tunnel junctions.

An increase of the junction normal state resistance R_n (decrease of critical current I_c) followed by further degradation of its characteristics at even higher temperatures, seemed to be a commonly agreed trend. General understanding behind the increase of the normal state resistance of Nb/Al-AlO_x/Nb junctions is that during the annealing at lower temperature range, below $250\ldots275\,^\circ C$, the tunnel barrier gets thicker either due to (additional) oxidation of the *Al* layer by chemisorbed oxygen [9], [14], or by adsorbed water molecules (hydroxyl groups) [5], [15]–[17]. This was supported by Raman spectroscopy study [18], showing decay of Al-OH peak and corresponding rise of Al-O peak as a result of Nb/Al-AlO_x/Nb junction annealing. At higher annealing temperatures, above $250\ldots275\,^\circ C$, AlO_x barrier apparently grows due to diffusion of oxygen through the junction's counter electrode [5], [6].

However, there are experimental facts, which do not fit the suggested trend and cannot be explained within the same approach. In the number of studies, unusual drop of R_n value of Nb/Al-AlO_x/Nb [10]–[12] and Al/Al-AlO_x/Al [13], [16], [19] junctions with annealing or aging has been observed.

In this study, partly reported earlier in [22], we experimentally observed a reduction of R_n of Nb/Al-AlO_x/Nb junctions with aging similarly to [10]–[12]. Unusually, this R_n reduction was accompanied with an increase of the subgap resistance, R_j . Furthermore, we observe the junction size affecting the R_n and R_j changes with aging. In addition, we experimentally detect a difference in persistence of the Nb/Al-AlO_x/Nb junctions recently fabricated and long time aged at room temperature. These phenomena hardly could find explanation within the concept of further oxidation of AlO_x barrier layer with adsorbed oxygen or water vapor. Below, we present a discussion in attempt to interpret all mentioned effects related to aging and annealing in terms of diffusion and stress-related processes in the vicinity of the tunnel barrier.

II. Experiment

The Nb/Al-AlO_x/Nb junctions studied in this work have been processed using dedicated equipment placed in class 100 clean-room environment. The junctions used in this studies were fabricated at the different stages of the SIS mixer development for the APEX Band 3 (385…500 GHz) receiver, which has recently been installed at the APEX telescope [20], [21]. The nominal junction areas were $A = 3\,\mu m^2$ (wafers R5.1, R6.1, R7.1, R8.2 and D1.2) and $A = 2\,\mu m^2$ (wafer D1.2), with the $\pm10\%$ typical spread of the junction size due to the processing-specific variation. The Nb/Al-AlO_x/Nb trilayer growth and processing parameters (please, see [22] for the details) were the same for all wafers discussed in the paper.

Each fabricated wafer contained 203 SIS mixer chips, out of which, 30 where connected to the wafer external contact pads, allowing dc characterization of the junctions before dicing wafer into single mixer chips. Each chip had a pair of junctions connected in parallel [20]. For junction characterization, we measured their current-voltage characteristics (IVC) at 4.2 K. Analyzing the recorded IVCs, we extracted the values of junction normal resistance, R_n and subgap resistance R_j (please, see [22] for the details). Normal state

Authors are with the Group for Advanced Receiver Development, Department of Earth and Space Sciences with Onsala Space Observatory, University of Technology, Gothenburg, SE 412 96, Sweden e-mail: Alexey.Pavolotsky@chalmers.se

resistance R_n corresponds to the resistance of normal electrons tunneling through AlO_x barrier at bias voltage higher than the junction superconducting gap voltage, V_g. R_n is considered as a measure of transparency of the tunnel barrier transparency. Another important parameter is the subgap resistance R_j, which corresponds to the resistance of quasiparticles tunneling through the barrier at bias voltages below V_g. There are very little of quasiparticles in niobium at 4.2 K. Therefore, the R_j value is very sensitive to the presence and quantity of the tunnel barrier defects and hence used as an indicator of the $Nb/Al\text{-}AlO_x/Nb$ tunnel junction quality.

As fabricated, all wafers demonstrated high-quality of the junctions and yield of about 90%. The junction parameters are $R_nA \simeq 20\,\Omega\,\mu m^2$, $R_j/R_n \simeq 15\ldots25$ and the superconducting gap voltage $V_g \simeq 2.87$ mV.

The aging of the wafers carried out in a controlled environment at room temperature $19\ldots23\,^\circ C$ in an air-conditioned laboratory room. The wafers were stored in standard anti-static trays and no additional measures were taken to protect the wafers from environmental factors during the storage period. The junction IVCs were recorded and changes in their R_n and R_j values due to aging were analyzed as a function of their area. Assuming the AlO_x barrier of $Nb/Al\text{-}AlO_x/Nb$ trilayer is uniform across the wafer area, the measure for the junction area is the recorded as-fabricated values of the R_n.

The junction annealing experiments were performed as a sequence of hot-plate baking steps at the range of temperatures $120\,^\circ C\ldots250\,^\circ C$ for 1 hour in the atmosphere of $42\pm2\%$ RH room air, with the temperature increased by a $10\,^\circ C$ -increment at each step. Each baking step followed by recording of the junction IVCs.

Some wafers were diced into the single chips right after the fabrication. Diced chips experienced aging under the same conditions, as described above.

III. Results and Discussion

Junctions from different wafers experience similar type of changes after long aging at room temperature. The normal state resistance of the junctions decays, which agrees with results reported in [10]–[12]. Furthermore, we have observed the junction size effect on R_n aging behavior, similar to that, reported in [12]. Fig. 1 depicts relative changes of the junction normal resistance, defined as $(R_n - R_{n0})/R_{n0}$, versus their normalized values of as-fabricated normal resistances R_{n0}/R_{n0}^{max} normalized by R_{n0}^{max}; here R_{n0}^{max} is maximum R_{n0} for the given wafer. There is a noticeable tendency that the more resistive junctions experience higher relative drop of the normal resistance. That indicates that the smaller area junctions exhibit relatively stronger decrease of their normal resistance due to aging as compared to the junctions of a bigger size on the same substrate. Interestingly, we did not observe similar aging behavior for the junctions located at the diced chips.

The reduction of R_n due to aging and the junction size effect are attempted to be explained in [10]–[12] by suggesting out-diffusion of hydrogen, trapped in the niobium electrodes during the junction fabricating. Following this explanation, one should expect similar behavior of the junction subgap resistance R_j with aging. However, we observe the tendency just opposite to the R_n changes: R_j increases with aging (Fig. 2). The wafers R5.1, 6.1 and R7.1 demonstrate a similar tendency of the R_j increasing and the results are earlier presented in [23]. It is worth to notice that the wafer D1.2 (measurements at Fig. 2) experienced about an order shorter aging, compared to the wafers R5.1, R6.1 and R7.1 ((measurements at Fig. 1)). While aging effect on R_j is clearly seen at the moderate aging times, the R_n changes are nearly not noticeable at shorter aging time. However, being exposed to annealing at $120\,^\circ C$ for 30 minutes, the junction normal resistance R_n changes, Fig. 3, showing the similar junction size effect and very much alike as after the long room temperature aging (Fig. 1). This

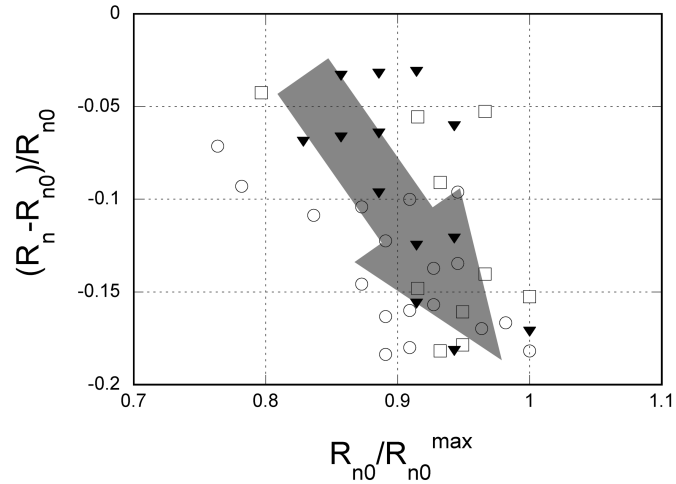

Fig. 1. Room temperature aging effect on the normal resistance of the junctions from wafers R5.1 (*circles*, aged for 655 days), R6.1 (*squares*, 597 days) and R7.1 (*triangles*, 428 days). R_{n0}, R_{n0}^{max}, and R_n - junction normal resistance as-deposited, maximal for the given wafer and after aging, correspondingly. Gray arrow illustrates the trend and guides eye.

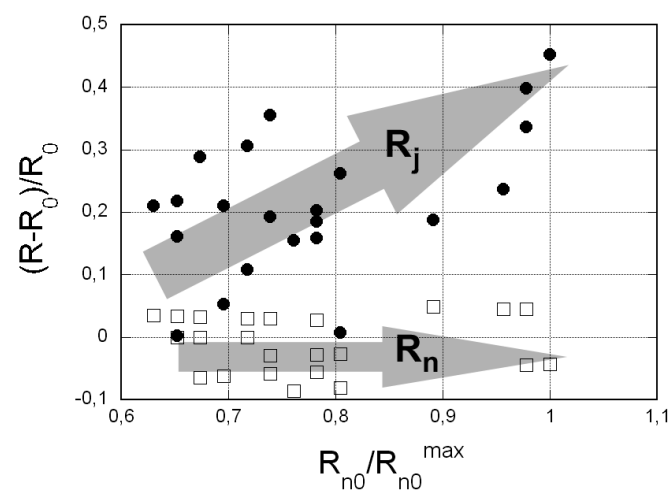

Fig. 2. Room temperature aging effect on the subgap (*circles*) and normal resistance (*squares*) of the junctions from the wafer D1.2 (aged for 63 days). R_{n0}^{max}, and R_n - junction normal resistance as-deposited, maximal for the given wafer and after aging, correspondingly. Gray arrows illustrate the trend and guide eye.

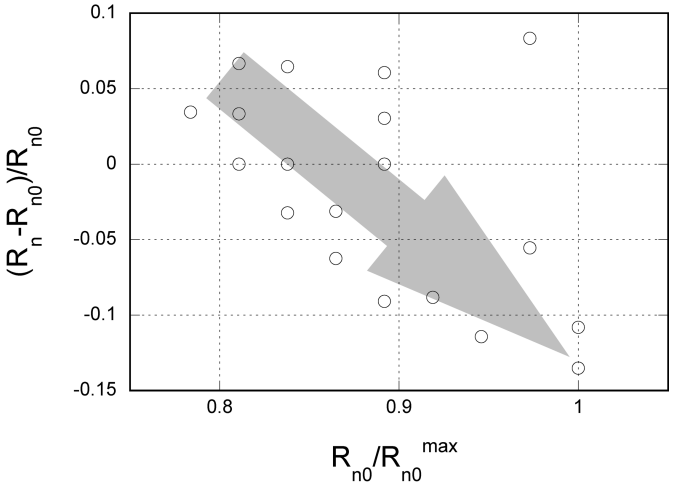

Fig. 3. Effect of annealing at $120\,^{\circ}C$ on the normal resistance of the $3\,\mu m$ size junctions from the wafer D1.2 (aged for 63 days before annealing). R_{n0}^{max}, and R_n - junction normal resistance as-deposited, maximal for the given wafer and after aging, correspondingly. Gray arrow illustrates the trend and guides eye.

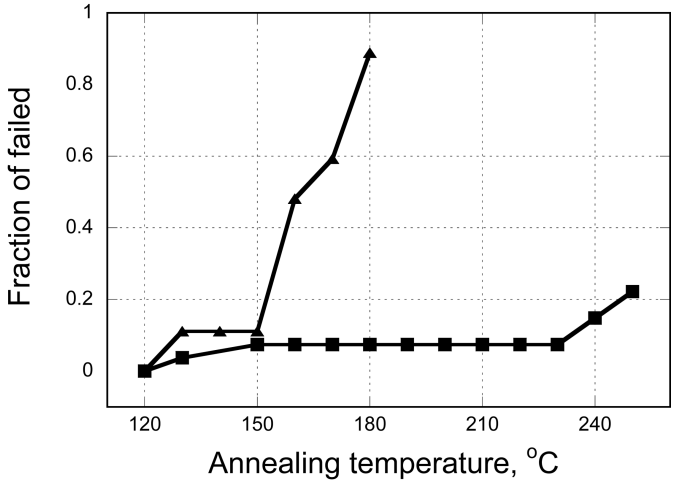

Fig. 4. Annealing temperature effect on the fraction of failed junctions, which experience long room temperature aging (wafer R8.2, aged for 391 days, *squares*), compared to that of junctions, experienced shorter aging (wafer D1.2, aged for 63 days, *triangles*).

points out to the fact that aging processes affecting R_j occur at a shorter time scale than those, causing R_n changes, and that fact could hardly be explain within the concept of hydrogen-induced aging effects.

After room temperature aging, the junctions were annealed at elevated temperatures, which effects their normal and sub-gap resistances as presented in [22] and, partially, in [23]. The changes, both for R_n and R_j, follow the same trend for the junctions experienced room temperature aging with different durations (batches R8.2 and D1.2). However, depending on the aging history, the junctions were able to survive annealing up to different temperatures. Fig. 4 compares the fraction of the failed junctions with respect to the annealing temperature for the wafers that were subject to pre-aging with different duration. Under the term "failed junction", we consider either a short-circuited junction or a junction with sufficiently degraded IVC. From this plot, we could suggest that the junctions subjected to a longer room temperature aging survive higher annealing temperature. Compared to the earlier presented data [5], [6], [8], [9], the longer pre-aged junctions (batch R8.2) demonstrate similar ability to persist annealing conditions. Worth mentioning though, the junctions used in the present work have substantially thinner tunnel barrier, then those reported in [5], [6], [8], [9]. This makes the junctions more susceptible to the intrinsic stress. This is discussed in more detail further in the paper.

Any direct studies of the processes in AlO_x tunnel barrier and adjacent to it layers are extremely difficult, as it is a structure of about one nm thick, sandwiched in between rather thick (200…500 nm) layers of niobium. However, in this discussion, we could greatly benefit from the recent results on *in-situ* studies of the growth kinetics and crystal state of the ultra-thin oxide film over the atomically clean single-crystal *Al* surfaces at the low temperatures between $80\,^{\circ}C$ and $380\,^{\circ}C$, ref. [24]–[26]. The conditions of the Al-oxide film growing in [24]–[26] largely resemble the conditions and thus the properties of the AlO_x tunnel barrier grown over the *Al* layer during fabrication of $Nb/Al\text{-}AlO_x/Nb$ junctions. The authors of these papers conclude that various processes of structural ordering in the oxygen sublattice of AlO_x , namely, an annihilation of the vacancy-type defects and even crystallization of initially amorphous oxide layer [24], [26], occur in the above mentioned interval of temperatures and AlO_x thickness about 1 nm. Applying these conclusions to the $Al\text{-}AlO_x$ layer of the tunnel barrier, we speculate that the same processes should certainly cause a decrease of the "leakage" component of the subgap current. This could explain the observed increase of R_j after room temperature aging. From the other hand, the structural ordering reduces the material volume [24], [26], and consequently causes thinning of the tunnel barrier and hence could explain a decrease of the R_n after a long aging.

Within the very same concept, the difference in the time scales of changes for both R_j and R_n could also be explained. The process of curing of minor structural defects that should lead to a raise of R_j , requires relatively little diffusion to occur, as discussed above. Whereas decreasing of R_n requires sufficient re-arrangement of the film structure and diffusion processes in the AlO_x film being developed in a very much longer time scale.

The studied room temperature aging of the $Nb/Al\text{-}AlO_x/Nb$ junctions occurs at noticeably lower temperature as compared to the conditions of ultra-thin oxide film growth presented in [24]–[26]. Nevertheless, we believe that even the aging effects could be explained through the AlO_x layer structure ordering. However in the case of the room temperature aging, a non-thermal enhancement of diffusion and consequent curing of the structural defects should exist. An indication of such non-thermal diffusion enhancement mechanism comes from observed dependance of R_n and R_j on junction area. The fact that the smaller junctions demonstrate a stronger aging effect points out to the intrinsic stress that always is accumulated in *Nb* film of the wiring layer during its growth. Our fabricating

process is calibrated in such way that the wiring layer *Nb* film typically characterized by slight compressive stress of about 100 MPa. Similarly, the fact that junctions on the diced chips did not demonstrate any noticeable aging changes also speaks for the role of the intrinsic stress in *Nb* film of the wiring layer. Sufficient fraction of stress is released during dicing, because long *Nb* wires connecting chips with anodization and testing terminals get cut.

In order to understand how the stress affects the tunnel junction, we assume perfect adhesion at the $Nb/Al\text{-}AlO_x/Nb$ $/Nb_{wiring}$ interfaces and account that the yield strength value is $100\ldots200$ MPa for a deposited *Al* material [27], that is comparable with the intrinsic stress of the niobium film. For *Al* , the room temperature corresponds to a moderate homologous temperature $\Theta_{Al} = T/T_m^{Al} \simeq 0.32$, where T_m^{Al} is melting temperature of *Al* . Altogether, this leads to a conclusion that the intrinsic stress in *Nb* wiring layer could be partly relaxed via creep deformation (stress relaxation process) of the aluminum layer of $Nb/Al\text{-}AlO_x/Nb$ trilayer at room temperature. This hypothesis is supported by an experimental observation of the stress relaxation in a free-standing microstructures made of sputtered *Al* films occured at room temperature, when originally loaded with a 50 MPa stress [28]. Furthermore, whatever mechanism of stress relaxation process takes place in *Al* layer of $Nb/Al\text{-}AlO_x/Nb$ trilayer, either diffusion creep [29], [30], or dislocation climb creep [30], [31], it should be associated with diffusional flows of vacancies in the *Al* layer. Vacancy flow in the vicinity of the AlO_x layer provides an additional diffusion path that in a non-thermal way enhances diffusion needed for structural ordering of AlO_x barrier layer.

Moreover, following the same concept, the difference in temperature dependence of the failed junctions ratio after annealing could be explained. The diffusion ordering of the AlO_x layer is far more slower than deformation (stress relaxation) of the *Al* layer . At higher annealing temperature, the *Al* layer deformation occurs quicker and tears AlO_x layer out, whereas the diffusion reconstruction cannot catch up creep of *Al* layer. Alternatively, a very long room temperature aging allows the major part of the *Al* layer relaxation to happen at low deformation speed, making the AlO_x layer reconstruction able to follow. Consequently, the annealing at elevated temperatures does not lead to tearing oxide layer out up to noticeably higher temperatures.

IV. Conclusion

We have studied long-term stability of $Nb/Al\text{-}AlO_x/Nb$ junctions of a $2\ldots3\,\mu m^2$ size, when stored at room temperature conditions. We observe reduction of the normal resistance R_n and increase of the subgap resistance R_j of the tested junctions as a result of room temperature aging. Changes of R_j occur at sufficiently shorter time scale than that of R_n . Room temperature storage (aging) effects for both R_n and R_j are subject to the junction size effect. Interestingly, junctions on the diced chips did not demonstrate any noticeable aging effects. Finally, we observed effect of aging history on the temperature dependence of the junction failure after consequent annealing.

We suggest that the observed junction aging and annealing behavior could be explained by diffusional ordering and structural reconstruction in the AlO_x layer. The diffusion driving the structural ordering and reconstruction of the AlO_x tunnel layer is enhanced due to the intrinsic stress relaxation (creep) processes in the underlying *Al* layer.

Acknowledgment

This work was partly supported by the Swedish Research Council under a grant. Authors are thankful to professor A. V. Lubenchenko for the fruitful discussions. Authors would like to acknowledge Dr. V. Desmaris for reading of the paper and the useful comments.

References

[1] Th. de Graauw, N.D. Whyborn, H. van de Stadt, G. Beaudin, D.A. Beintema, V. Belitsky, et.al., "Heterodyne instrument for FIRST (HIFI): Preliminary design," *Proc. SPIE*, vol. 3357, pp. 336 - 347, 1998.

[2] R. S. Booth, "ALMA, the Atacama Large Millimetre Array," *Proceedings of the Conference "Darwin and Astronomy — The Infrared space Interferometer"*, Stockholm, Sweden, 17 - 19 November 1999, European Space Agency, 2000, ESA SP, vol. 451, ISBN 92–9092-645-7., pp.107 - 114.

[3] J. M. Rowell, M. Gurvitch, J. Geerk, "Modification of tunneling barriers on Nb by a few monolayers of Al," *Physical Review B*, vol. 24, No. 4, pp. 2278 - 2281, 1981.

[4] M. Gurvitch M. A. Washington and H. A. Huggins, "High quality refractory Josephson tunnel junctions utilizing thin aluminium layers," *Applied Physics Letters*, vol. 42, No. 5, pp. 472 - 474, 1983.

[5] J. V. Gates, M. A. Washington and M. Gurvitch, "Critical current uniformity and stability of Nb/Al-oxide-Nb Josephson junctions," *Journal of Applied Physics*, vol. 55, No. 5, pp. 1419 - 1421, 1984.

[6] T. Shiota, T. Imamura, and S. Hasuo, "Fabrication of high quality $Nb/Al\text{-}AlO_x/Nb$ josephson junctions: III – Annealing Stability of AlO_x tunneling barriers," *IEEE Transactions on Applied Superconductivity*, vol. 2, No. 4, pp. 222 - 227, 1992.

[7] S. Morohashi, Y. Kataoka, T. Imamura, and S. Hasuo, "Secondary ion mass spectrometry study for Josephson junction with $Nb/Al\text{-}AlO_x/Nb$ structure," *Applied Physics Letters*, vol. 62, No. 10, pp. 1164 - 1166, 1993.

[8] A. Oliva and R. Monaco, "Annealing properties of high quality $Nb/Al\text{-}AlO_x/Nb$ tunnel junctions," *IEEE Transactions on Applied Superconductivity*, vol. 4, No. 1, pp. 25 - 32, 1994.

[9] T. Lehnert, D. Billon, C. Grassl, and K. H. Gundlach, "Thermal annealing properties of $Nb/Al\text{-}AlO_x/Nb$ tunnel junctions," *Journal of Applied Physics*, vol. 72, No. 7, pp. 3165 - 3168, 1992.

[10] S. K. Tolpygo and D. Amparo, "Fabrication-process-induced variations of $Nb/Al\text{-}AlO_x/Nb$ josephson junctions in superconductor integrated circuits," *Superconducting Science and Technology*, vol. 23, 034024, 2010.

[11] K. Hinode, T. Satoh, S. Nagasawa, and M. Hidaka, "Hydrogen-inclusion-induced critical current deviation of $Nb/Al\text{-}AlO_x/Nb$ josephson junctions in superconducting integrated circuits," *IEEE Transactions on Applied Superconductivity*, vol. 19, No. 3, pp. 131 - 134, 2009.

[12] K. Hinode, T. Satoh, S. Nagasawa, and M. Hidaka, "Origin of hydrogen-inclusion-induced critical current deviation in $Nb/Al\text{-}AlO_x/Nb$ josephson junctions," *Journal of Applied Physics*, vol. 107, 073906, 2010.

[13] H. Scherer, Th. Weimann, A. B. Zorin, and J. Niemeyer, "The effect of thermal annealing on the properties of $Al/Al\text{-}AlO_x/Al$ single electron tunneling transistors," *Journal of Applied Physics*, vol. 90, No. 5, pp. 2528 - 2532, 2001.

[14] P. J. Koppinen, L.,M. Väistö, and I.,J. Maasilta, "Complete stabilization and improvement of the characteristics of tunnel junctions by thermal annealing," *Applied Physics Letters*, vol. 90, 053503, 2007.

[15] A. L. Geiger, B. S. Chandrasekhar, J. G. Adler, "Inelastic electron tunneling in Al-Al-Oxide-Metal systems," *Physical Review*, vol. 188, No. 3, pp. 1130 - 1138, 1969.

[16] M. K. Konkin and J. G. Adler, "Annealing effects in tunnel junctions (thermal annealing)," *Journal of Applied Physics*, vol. 50, No. 12, pp. 8125 - 8128, 1979.

[17] M. K. Konkin and J. G. Adler, "Annealing effects in tunnel junctions (voltage annealing)," *Journal of Applied Physics*, vol. 51, No. 10, pp. 5450 - 5454, 1980.

[18] S. Morohashi, "Raman spectroscopic study of $Nb/Al\text{-}AlO_x/Nb$ josephson junctions," *Japaneze Journal of Applied Phisics*, vol. 33, Part 2, No. 2A, pp. L170 - L172, 1994.

[19] T. Holmqvist, M. Meschke ,and J. P. Pekola, "Double oxidation scheme for tunnel junction fabrication," *Journal of Vacuum Science and Technology B*, vol. B26, No. 1, pp. 28 - 31, 2008.

[20] R. R. Monje, V. Belitsky, V. Vassilev, A. Pavolotsky, I. Lapkin, V. Desmaris, D. Meledin, D. Henke, D. Dochev, "A 0.5 THz Sideband Separation SIS Mixer for APEX Telescope," *19th International symposium on space terahertz technology*, April 28 - 30, Groningen, The Netherlands, pp. 439 - 443, 2008.

[21] Latest status and technical details at *http://gard04.rss.chalmers.se/APEX_web/SHeFI.htm*

[22] A. B. Pavolotsky, D. Dochev, V. Belitsky. "Aging- and annealing-induced variation in $Nb/Al\text{-}AlO_x/Nb$ tunnel junction properties," *Journal of Applied Physics*, vol. 109, No. 2, 024502, 2011.

[23] D. Dochev, A. B. Pavolotsky, Z. Lai and V. Belitsky, "The influence of aging and annealing on the properties of $Nb/Al\text{-}AlO_x/Nb$ tunnel junctions," *Journal of Physics: Conference Series*, vol. 234, 042006, 2010.

[24] P. C. Snijders, L. P. H. Jeurgens, W. G. Sloof, "Structural ordering of ultra-thin, amorphous aluminium-oxide films," *Surface Science*, vol. 589, pp. 98 105, 2005.

[25] F. Reichel, L. P. H. Jeurgens, E. J. Mittemeijer, "The effect of substrate orientation on the kinetics of ultra-thin oxide-film growth on Al single crystals," *Acta Materialia*, vol. 56, pp. 2897 2907, 2008.

[26] F. Reichel, L. P. H. Jeurgens, G. Richter, and E. J. Mittemeijer, "Amorphous versus crystalline state for ultrathin Al_2O_3 overgrowths on *Al* substrates," *Journal of Applied Physics*, vol. 103, 093515, 2008.

[27] F.-J. Lee, P. Zhang and J. C. Bravman, "Study on the strength and elongation of free-standing Al beams for microelectromechanical systems applications," *Applied Physics Letters*, vol. 84, pp. 915 - 917, 2004.

[28] F.-J. Lee, G. Cornella and J. C. Bravman, "Stress relaxation of of free-standing Al beams for microelectromechanical systems applications," *Applied Physics Letters*, vol. 76, pp. 3415 - 3417, 2000.

[29] C. Herring, "Diffusional viscosity of a polycrystalline solid," *Journal of Applied Physics*, vol. 21, pp. 437 - 445, 1950.

[30] B. Ya. Pines, "Diffusion and the mechanical properties of solids," *Soviet Physics Uspekhi*, vol. 5, pp. 251 - 271, 1962.

[31] J. Weertman, "Theory of steady-state creep based dislocation climb," *Journal of Applied Physics*, vol. 26, pp. 1213 - 1217, 1955.